



Tenofovir Disoproxil Fumarate Release From Glutaraldehyde Cross-Linked Chitosan/B-Cyclodextrin Hydrogel

Gluteraldehit Çapraz Bağlı Kitosan/B-Siklodekstrin Hidrojelinden Tenofovir Disoproksil Fumarat Salımı

Nuh Yaman¹, Sevil Erdoğan^{2*}, Betül Taşdelen³

¹Biotechnology and Genetic Department, Institute of Science, Trakya University, Edirne/Turkey.

²Laborant and Veterinary Programme, Keşan Vocational College, Trakya University, Keşan, Edirne/Turkey.

³Biomedical Engineering Department, Çorlu Engineering Faculty, Namık Kemal University, Tekirdağ, Turkey.

ABSTRACT

In this study, chitosan was produced from crayfish *Astacus leptodactylus*, and then it was used to synthesize chitosan-graft- β -cyclodextrin (CS-g- β -CD) hydrogel. The produced chitosan (CS) and the synthesized CS-g- β -CD hydrogel were characterized using a Fourier Transform Infrared Spectroscopy (FTIR), Proton Nuclear Magnetic Resonance Spectroscopy ($^1\text{H-NMR}$), X-ray Diffraction (XRD), and Scanning Electron Microscopy (SEM). Tenofovir disoproxil fumarate (TDF) was used as a model to investigate the antiviral drug release properties of the CS-g- β -CD hydrogel. The synthesized hydrogel had an almost homogeneous pore structure and a high swelling capacity which increases depending on the amount of β -Cyclodextrin (β -CD). The drug-loaded CS-g- β -CD hydrogels were examined by XRD, $^1\text{H-NMR}$, and SEM analyses. Seventy-three percent of the TDF loaded on the synthesized hydrogels was released into phosphate-buffered saline (PBS) solution at 37°C. The drug release behavior of all prepared CS-g- β -CD hydrogels fitted the Korsmeyer-Peppas model. The addition of β -CD into the gel improved the swelling ability and TDF release of the CS-g- β -CD hydrogel system.

Key Words

Crayfish chitosan, degree of deacetylation, antiviral drug, drug release.

Öz

Bu çalışmada, kerevit *Astacus leptodactylus*'tan kitosan üretildi ve daha sonra kitosan-graft- β -siklodekstrin (CS-g- β -CD) hidrojelinin sentezinde kullanıldı. Üretilen kitosan (CS) ve sentezlenen CS-g- β -CD hidrojeli Fourier Dönüşümlü Kızılötesi Spektroskopisi (FTIR), Proton Nükleer Manyetik Rezonans Spektroskopisi ($^1\text{H-NMR}$), X-ışını Kırınımı (XRD) ve Taramalı Elektron Mikroskopu (SEM) kullanılarak karakterize edildi. Tenofovir disoproksil fumarat (TDF), CS-g- β -CD hidrojelinin antiviral ilaç salma özelliklerini araştırmak için model ilaç olarak kullanıldı. Sentezlenen hidrojel hemen hemen homojen bir gözenek yapısına ve β -Siklodekstrin (β -CD) miktarına bağlı olarak artan yüksek şişme kapasitesine sahipti. İlaç yüklü CS-g- β -CD hidrojellerinin yapısı XRD, $^1\text{H-NMR}$ ve SEM analizleriyle incelendi. Sentezlenen hidrojellere yüklenen TDF'nin yüzde yetmiş üçü 37°C'de fosfat tamponlu tuz (PBS) çözeltisine salındı. Hazırlanan tüm CS-g- β -CD hidrojellerinin ilaç salım davranışı Korsmeyer-Peppas modeline uyum sağladı. Jel içerisine β -CD eklenmesi CS-g- β -CD hidrojel sisteminin şişme kabiliyetini ve TDF salımını arttırdı.

Anahtar Kelimeler

Kerevit kitosanı, deasetilasyon derecesi, antiviral ilaç, ilaç salımı.

Article History: Aug 2, 2023; Revised: Nov 23, 2023; Accepted: Dec 9, 2023; Available Online: Feb 8, 2024.

DOI: <https://doi.org/10.15671/hjbc.1335348>

Correspondence to: S. Erdoğan, Laborant and Veterinary Programme, Keşan Vocational College, Trakya University, 22800 Keşan, Edirne/Turkey.

E-Mail: sevilerdogan@trakya.edu.tr

INTRODUCTION

Viral infections lead to economic and social losses, especially to human health, and constitute a global burden [1]. HIV virus, which lead to Acquired Immunodeficiency Syndrome (AIDS), is a life-threatening infection that impairs the immune system and reduce its resistance to infections and diseases [2]. Hepatitis B virus causes both acute and chronic disease by attacking the liver, thus increasing the risk of death from cirrhosis and liver cancer [3]. It is estimated that the people who lived with chronic hepatitis B infection were 296 million in 2019 and 1.5 million people are infected each year [3]. The Joint United Nations Programme on HIV/AIDS (UNAIDS) [4] reported that there were 37.7 million AIDS patients worldwide in 2020, and 1.5 million people were newly infected with HIV in that year. Since the HIV cannot be expelled from the body once it enters the body, one of the main goals of treatment is to prevent the proliferation of HIV in the body [2]. Likewise, most people who start hepatitis B treatment have to continue the treatment for life. Since these viral diseases require long-term treatment, it is a necessity for drug treatments to be effective and safe [5].

Tenofovir disoproxil fumarate (TDF), which is a prodrug of Tenofovir [6], was approved for the treatment of HIV (2001) and chronic Hepatitis B (2008) by the FDA [2,5]. TDF functions as a reverse transcriptase inhibitor for HIV-1 and Hepatitis B viruses [6-8]. It is recommended by WHO for use to suppress the Hepatitis B virus and in the primary treatment of HIV [3]. The oral bioavailability of TDF ranges from 25% to 40% [5]. TDF and intravenous Tenofovir cause bone and kidney toxicity when administered at high doses in toxicology studies [2,5,6]. Likewise, the bioavailability of many of the antiviral drugs in the body after being taken by the patient is quite weak [9]. For example, the antiviral drug acyclovir, which has poor solubility, low oral bioavailability, and short half-life has to be administered both several times a day and at high doses [10]. This situation can be overcome with controlled release systems that reduce the dosage frequency, toxicity and side effects of the drug. Research has shown that these deficiencies in antiviral drugs can be resolved through polymeric drug delivery systems [11].

Hydrogels can suck in large amounts of water and physiological fluids thanks to their network structure, and remain insoluble in aqueous solutions [12,13]. Hydrogels

swell by absorbing a huge amount of fluid and, in this state, they are rubbery soft and tend to show excellent similarity to living tissues [11]. Hydrogels made of polysaccharides are used as drug carriers in pharmaceutical applications thanks to their biocompatible, biodegradable, and non-toxic properties, and the controlled release ability [13-15]. In this study, natural polysaccharides, chitosan (CS) and β -cyclodextrin (β -CD) were used to synthesize the hydrogel.

CS is a biopolysaccharide of interest in the pharmaceutical industry as a polymeric drugs carrier thanks to its non-toxicity, low allergenicity, biocompatibility, biodegradability, bioactivity and mucoadhesiveness [11,16-18]. CS has a very high water-retention capacity thanks to its hydrophilic structure, making it an excellent polymer for drug delivery [17]. It also forms micelles, forming a hydrophobic center for hydrophobic drugs [19]. Thus, hydrophobic drugs are preserved in the core and gain increased solubility and bioavailability [16]. In addition, CS helps drugs to cross biological barriers more easily [15]. Recent studies have drawn attention to the CS nanoparticles in developing a drug delivery system that will increase the therapeutic efficacy of antiviral agents and reduce the therapeutic dose [20]. Although there are many studies on the delivery of various drugs through CS hydrogels, there have been few studies on the delivery of antiviral drugs with low bioavailability by the hydrogel system. Therefore, this study focused on the release of the antiviral drug TDF from the CS-based hydrogel system.

Cyclodextrins are oligomers of ring-shaped α -(1,4) linked-glycopyranosylline synthesized by enzymatic conversion of starch [21]. Natural cyclodextrins carry 6 (α -CD), 7 (β -CDs) or 8 (γ -CD) glucose units [22]. Cyclodextrins are hydrophilic on the outside and have a hydrophobic inner cavity providing shelter for hydrophobic molecules [23]. Cyclodextrins are biological molecules that gain importance as drug carriers in the pharmaceutical applications thanks to their capability to make complexes with hydrophobic molecules [24]. In addition, cyclodextrins are biocompatible, have low toxicity, and do not elicit an immune response [21,22]. Cyclodextrins are preferred in drug applications to improve drug stability, solubility, and drug absorption, control drug release, and diminish systemic toxicity [24]. β -CD is the most preferred cyclodextrin derivative due to its potential to form inclusion complexes with hydrophobic drugs, the appropriate cavity size for hydrophobic drugs, and low

toxicity [23,25,26]. β -cyclodextrin is utilized to improve the bioavailability and solubility of hydrophobic drugs [27]. In addition, there are some findings that the addition of β -cyclodextrin to the chitosan hydrogel improves the pH, gelling, viscosity, and drug release behavior of the hydrogel [26]. Several studies have been published on the delivery of antiviral, cardiovascular, and antibiotic drugs via β -cyclodextrin-based hydrogels [27-29].

This study aims to synthesize and characterize the chitosan-graft- β -cyclodextrin (CS-g- β -CD) hydrogel consisting of biocompatible and biodegradable polymers and to examine TDF release behavior, a model antiviral drug of this hydrogel.

MATERIALS and METHODS

Materials

Chitosan was produced from the crayfish *Astacus leptodactylus*, which was caught by the fishermen in July 2020 from the Kocahidir Dam Lake (Edirne/Turkey). 2-Hydroxypropyl- β -cyclodextrin (HP- β -CD) (mean Mw ca. 1460, Pcode: 102363932, Slovakia), Glutaraldehyde (50% aqueous solution, Pcode: 1003100323, USA), and phosphate-buffered saline (PBS) (Pcode: 1003090549, P4417-100 tablets) were purchased from Sigma Aldrich.

TDF used in the drug release studies was obtained from Nobel İlaç San. ve Tic. A.Ş. (Turkey) company (Figure 1). All chemicals from the analytical reagent class were used without any purification.

CS Production

After washing and cleaning the crayfish shells, they were dried at 37°C for one week. Later, crayfish shells were pulverized in a blender. The isolation of chitin was carried out by going through the demineralization and deproteinization stages, respectively. Firstly, the ground shells were treated with 2M 450 mL HCl (v/v) by stirring in a magnetic stirrer at 80°C and 700 rpm for 6 hours. Then, it was washed with distilled water until reaching pH 7. Next, the filtrate was refluxed with 2M 400 mL NaOH solution (w/v) at 80°C and 800 rpm of stirring speed for 24 hours. After, it is filtered through filter paper by washing with deionized water for reaching the neutral pH. Finally, the chitin obtained was dried at 55°C for a few days.

CS was obtained from crayfish chitin by deacetylation process. The crayfish chitin was treated with 130 mL 70% NaOH (w/v) at 160°C for 3 hours. Afterwards, it was filtered and washed in order to reach pH 7. Then obtained CS was dried at 50°C for a few days.

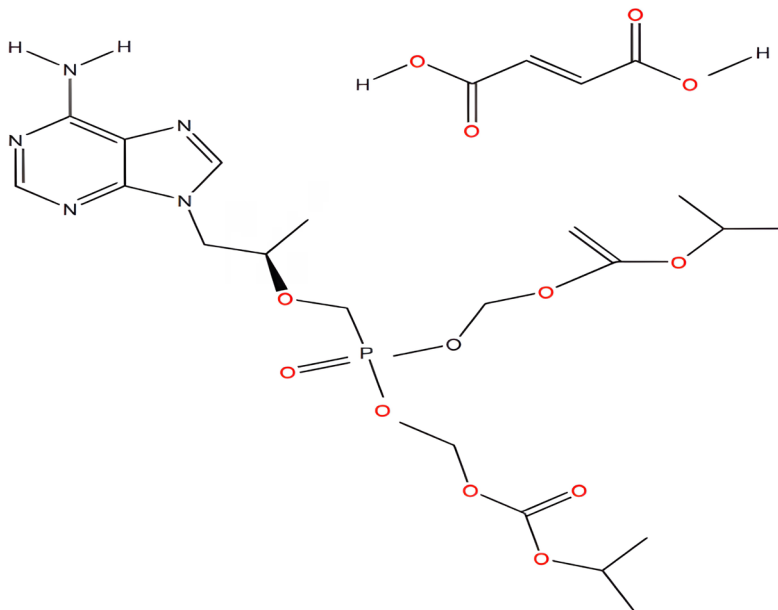


Figure 1. Tenofovir disoproxil fumarate.

CS-g-β-CD Hydrogel Synthesis

Preliminary experiments were performed using different concentrations of the β-CD (0 g (gel G0), 0.02 g (gel G1), 0.03 g (gel G2) and 0.04 g (gel G3)) and glutaraldehyde crosslinker (0.4%) until the optimum CS-g-β-CD hydrogel system was obtained. Thus, optimum concentrations of the β-CD was determined. First, 0.1 g of the crayfish CS was dissolved in a 1% acetic acid (CH₃COOH) solution of 10 mL by stirring on the magnetic stirrer at 25°C and 500 rpm, for 10 minutes. Then, 0.04 g of the β-CD was dissolved in 1% CH₃COOH and immediately added to the gel mixture. Next, a 0.4% glutaraldehyde solution of 2.5 mL was added to the obtained CS solution as a crosslinker and mixed again for 10 minutes. After that, the viscous gel mixture was poured into small glass tubes with an inner diameter of 5 mm and a length of 10 cm and kept in a deep freezer at -20°C for 48 hours, and freeze gelation technique was applied. Finally, the CS-g-β-CD hydrogel was produced as cylindrical rods by breaking the glass tube.

Physicochemical Characterization of Crayfish CS and Synthesized Hydrogels

Hydrogen (H), Carbon (C), and Nitrogen (N) percentages of the CS produced from crayfish shells were measured using Thermo Finnigan elemental analyzer (Flash EA 1112 Series). The formula below was applied for the calculation of the degree of deacetylation (DD) of the crayfish CS [19].

$$DD = \left[\frac{\frac{C}{N} - 5.14}{1.72} \right] \times 100 \quad (1)$$

The viscosity-average molecular weight (Mw) of the crayfish CS was measured using a Ubbelohde type viscometer. Flow times in the Ubbelohde viscometer of CS solutions prepared at 1%, 0.8%, 0.6%, 0.5% and 0.4% (w/v) concentrations using a solvent containing CH₃COOH (0.1 M) and NaCl (0.2 M) (1:1, v/v) were recorded. Mw determination was performed at 25°C. The recorded values were replaced in the Mark – Houwink equation and the Mw of the crayfish CS was calculated [30].

$$[\eta] = kMv^\alpha \quad (2)$$

[η]; represents the intrinsic viscosity

Mv; represents the viscosity-average molecular weight of the CS

k and α; represents Mark – Houwink – Sakurada constants. k= 1.81 x 10⁻³ and α = 0.93.

In order to identify the crayfish CS and copolymer hydrogels, Fourier Transform Infrared Spectrometry (FTIR) was used. The FTIR spectra were generated in the Perkin Elmer FTIR device (ATR) in the range of 400-4000 cm⁻¹.

The morphological and topographical features of the produced CS and the synthesized hydrogels were visualized with a Scanning Electron Microscope (SEM) (EVO LS 10) at various magnifications such as 500X and 1000X. Samples were gold plated prior to analysis.

X-Ray Diffraction (XRD) patterns of the synthesized hydrogels were produced using an Bruker Smart Apex II Quazar brand X-ray diffractometer and an APEX II CCD detector at 2θ, 40 kV, and 40 mA, with a diffraction angle of 5-50°.

Proton Nuclear Magnetic Resonance Spectroscopy (¹H-NMR) was performed to observe polymer-drug complex formation in the drug-loaded hydrogels. Analysis was performed with a Bruker 500 NMR (Avance Neo Bruker console) spectrometer. ¹H-NMR spectroscopies of the hydrogels were recorded at room temperature using deuteriochloroform (CDCl₃) as solvent.

Functionality Tests of Synthesized Hydrogels

Gelation Measurements of Hydrogels

The synthesized hydrogels were dried at room temperature and their initial weights (W₀) were measured. Then, the gels were kept in distilled water to remove any un-gelled parts and impurities. After this process, the gels were dried at 37°C. The final weights (W_g) were then measured. Gelation (%) was determined by the formula given below:

$$\text{Gelation (\%)} = \frac{W_g}{W_0} \times 100 \quad (3)$$

While the W_g refers to the weight after extraction, W₀ refers to the weight before extraction.

Swelling Measurements of Hydrogels

The prepared dry hydrogels were soaked in vials filled with distilled water at 25°C. Swelling was allowed to continue until an equilibrium swelling state was reached. The change in mass swelling percentage was gravimetrically measured as a function of time using the formula given below by dividing the water retained in the hydrogel at any fixed time by the dry hydrogel weight.

$$\text{Mass Swelling (\%)} = \frac{[m_t - m_0]}{m_0} \times 100 \quad (4)$$

$$\text{Equilibrium Mass Swelling (S}_{eq}\text{\%)} = \frac{(m_{\infty} - m_0)}{m_0} \times 100 \quad (5)$$

while the m_0 represents the mass of the dry gel, m_{∞} and m_t represent the swollen gel mass at equilibrium and time t , respectively.

Establishment of Standard Calibration Curves of the Antiviral Drug

TDF (1 mg) was dissolved in a solution containing an equal amount of distilled water (5 mL) and methanol (5 mL). The absorbance of the TDF solution was measured using a Shimadzu UV-1900i spectrometer between 200-400 nm wavelength, and the maximum absorbance value (λ_{max}) was determined as 261 nm. Afterwards, the drug solutions at the concentrations of 10, 20, 30, 40, and 50 ppm were prepared and their absorbance at 261 nm were determined and a calibration graph was drawn.

Drug Release

Since drug TDF was loaded on the CS-g- β -CD hydrogels during gel synthesis (in situ loading), all the amount of the drug was entrapped into the cryogel with maximum drug loading efficiency [31]. In order to load the model drug on the hydrogel, a certain quantity of the drug (20, 30, 40 mg) was put into the CS- β -CD solution and mixed for 15 minutes before the addition of the glutaraldehyde solution as mentioned in CS-g- β -CD hydrogel synthesis part. For drug release, the loaded gel was added into the PBS buffer solution at 37°C and pH 7.4. At certain intervals, 3 mL of the solution that the drug released was drawn in order to measure spectroscopically at 261 nm in a UV-VIS spectrophotometer and again poured into the same vial to keep the liquid volume constant. A calibration curve was used to calculate the amounts of the released drug.

In order to determine the amount of the tenofovir disoproxil fumarate released from the CS-g- β -CD hydrogel depending on the concentration, 0.5, 1, 2, 4, 6, 8 and 10 ppm reference concentrations of the drug solutions were prepared, and their absorbances were read at 261 nm. The regression equation was determined by creating a calibration curve.

Equations 6-9 were applied for the antiviral drug release kinetics of all the prepared hydrogels, and the results evaluated by Korsmeyer-Peppas, zero-order, first-order and Higuchi models.

For zero-order kinetics [32]

$$\frac{M_t}{M_{\infty}} = K_0 t \quad (6)$$

K_0 is the zero-order release constant.

For first-order kinetics [33]

$$\ln\left(1 - \frac{M_t}{M_{\infty}}\right) = -K_1 t \quad (7)$$

K_1 is the first-order release constant.

For Higuchi model [34]

$$F = K_2 t^{1/2} \quad (8)$$

K_2 is the Higuchi constant.

For Korsmeyer-Peppas model [35]

$$F = \frac{M_t}{M_{\infty}} = k t^n \quad (9)$$

k represents a constant, n represents the diffusional exponent, M_{∞} represents the maximum drug amount absorbed, M_t represents the amount of absorbed at time t . For cylindrical samples, $n=0.45$ represents a Fickian diffusion, $0.45 < n < 0.89$ represents a non-Fickian diffusion, and $n < 0.45$ represents a pseudo-Fickian diffusion [36].

RESULTS and DISCUSSION

Characterization Analysis Results of the CS Obtained from Crayfish *A. leptodactylus*

FTIR spectra of the crayfish CS are presented in the section FTIR Analysis Result of Hydrogels. The FTIR spectra of the crayfish CS exhibit similar absorption peaks to

those of commercial CS reported by Kaya et al. [37]. In addition, the absorption spectra observed in this study are similar to the absorption spectra of crayfish CS reported by Erdoğan [38]. The broad overlapping peak in the region of 3000–3600 cm^{-1} is referred to as the vibrations of N–H and O–H groups in CS [39]. Michailidou et al. [39] also observed other absorption bands for CS at 1651 cm^{-1} and 1567 cm^{-1} , at 1421 cm^{-1} , at 1154 cm^{-1} and at 1077 cm^{-1} representing the amide I and II, vibrations of C–H and O–H groups, the symmetrical stretching of the anti-C–O–C, and C–O, respectively. The observation of characteristic amide peaks identifying CS in the FTIR spectra of CS produced from *A. leptodactylus*, confirmed that the CS was successfully produced from the crayfish shells.

The viscosity average Mw of the CS obtained from crayfish *A. leptodactylus* was determined as 17.82 kDa. Gomes et al. [40] obtained highly pure β -CS at molecular weights of 206 and 294 kDa from the squid species *Loligo opalescens*. Joseph et al. [41] reported that the Mw of CS varies between 200 and 1000 kDa, depending on the chitosan source. The authors classified CS with a Mw below 300 kDa as low Mw CS, and above 300 kDa as high Mw CS. Considering this study, the crayfish CS is

in the low Mw CS class. Mw is a major component that affects the solubility of the polymer, as well as degree of acetylation, crystallinity, pH and temperature [42]. Low Mw CS is more convenient for the distribution of protein-based drugs and it facilitates the absorption of bioactive compounds and CS-based drugs from the intestine [41].

By elemental analysis, C%, N%, and H% contents of the crayfish CS were determined as 40.62%, 7.13% and 6.74%, respectively. Based on these values, the DD of the crayfish CS was determined as 32.3%. The DD is the number of D-glucosamine units in the CS polymer and a key factor that crucially affects the solubility, biological activity and chemical properties of CS [16,43]. Aranaz et al. [42] state that the CS sample having a DD of 49% and homogeneous deacetylation is water-soluble. While the CS with a DD between 70-99% is classified as high DD CS, the CS with a DD of 55-70% is classified as low DD [41]. The authors noted that a DD higher than 70% is optimal for drug delivery applications. The DD affects the heat-sensitivity of the CS hydrogel. The optimal DD for the heat-sensitive chitosan-ab-glycerophosphate (CS-ab-GP) hydrogel was found to be 75.4% [44]. According to this classification, the crayfish CS is in the class of CS with low DD.

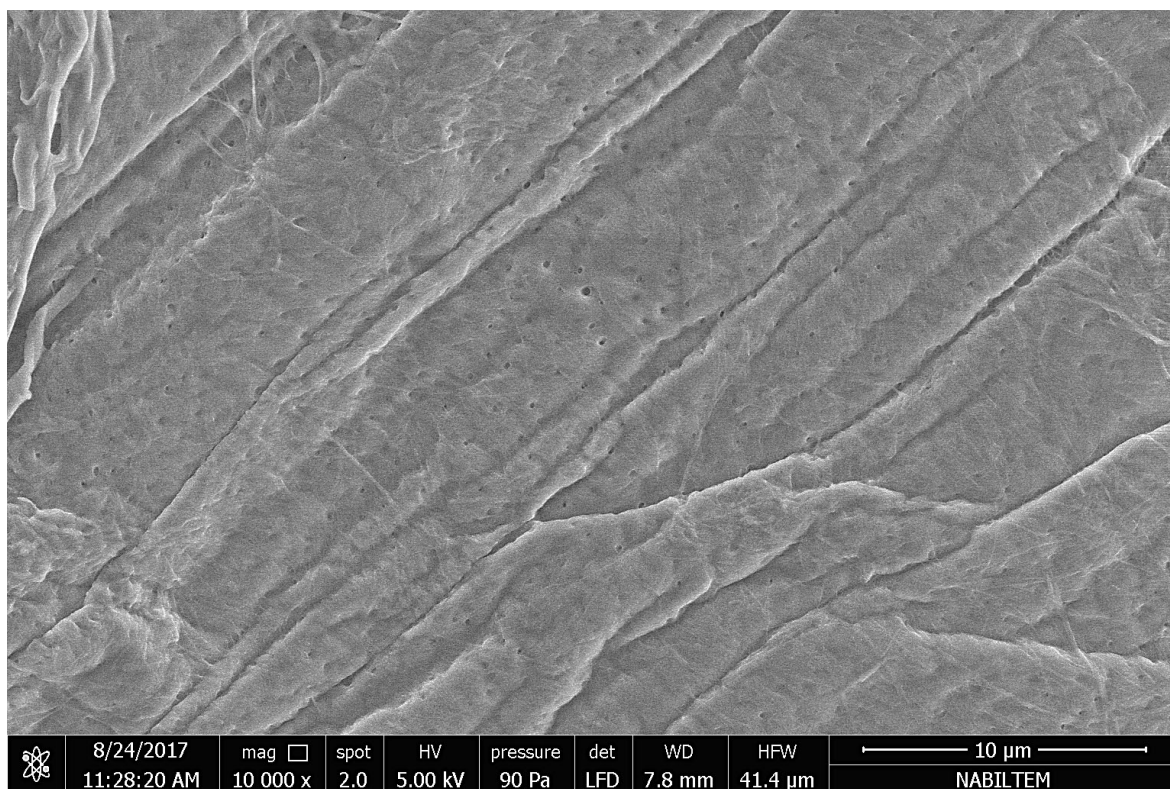


Figure 2. Surface morphology of the CS obtained from the crayfish *A. leptodactylus*.

The surface properties of the CS obtained from the crayfish *A. leptodactylus* were examined by SEM and presented in Figure 2. SEM analysis reveals that the crayfish CS exhibits folded and wrinkled structure, and also has fibers and homogeneously dispersed pores of almost equal size. The surface morphology of the crayfish CS is similar to that of CS from blue crab [37].

Characterization Analysis Results of the Synthesized CS-g- β -CD Hydrogels

FTIR Analysis Results of Hydrogels

The FTIR spectra of the β -CD, CS, and the synthesized CS-g- β -CD hydrogel are shown in Figure 3. The FTIR spectra of the crayfish CS was discussed above. The presence of distinctive bands at 1647 cm^{-1} and 1584 cm^{-1} corresponding to the amide I and amide II specific to CS were observed in the FTIR spectra (Figure 3a). Typical bands of saccharides were observed at 3329 cm^{-1} (stretching of O-H), 2924 cm^{-1} (stretching of C-H), 1647 cm^{-1} (bending of O-H), 1152 cm^{-1} (vibration of C-O), and 1023 cm^{-1} (stretching of C-O-C) in the absorption spectra of β -CD (Figure 3b). In another study, prominent absorption peaks of β -CD were observed at 2929 cm^{-1} (stretching of C-H), 1645 cm^{-1} (bending of H-O-H), 1157 cm^{-1} (stretching of C-O), and 1031 cm^{-1} (stretching of C-O-C) [45]. The CS and the β -CD both exhibited similar absorption bands in the FTIR spectra since they are both in carbohydrate structure. Paun et al. [46] stated that the IR spectra of the composite CS-g- β -CD membrane were almost identical to that of the CS membrane due to the low contents of β -CD. Similar results were observed in this study as well. The FTIR spectra of the synthesized hydrogel revealed the interaction between the raw polymers (Figure 3c). The intensity of the peaks observed at 1647 cm^{-1} in the spectra of CS decreased and this band shifted to 1636 cm^{-1} in the spectra of the hydrogel. Another absorption peak observed at 1584 cm^{-1} in the CS spectra shifted to 1549 cm^{-1} in the IR spectra of the hydrogel. The intensity of the band responsible for the NH bending of the uncrosslinked CS was reported to decrease to 1636 cm^{-1} in the absorption spectra of the CS hydrogel developed for the delivery of antiviral drug megosine [47]. The authors noted that the movement of this absorption band to a lower wavelength indicates crosslinking in the gel. In addition to these, the intensity of the peaks observed at around

1417 cm^{-1} and 1456 cm^{-1} in the spectra of the crayfish CS and the β -CD, respectively decreased. An intense peak around 1405 cm^{-1} was recorded in the FTIR spectra of the synthesized hydrogel. The peaks at 1380 cm^{-1} and 1257 cm^{-1} in the spectra of the synthesized hydrogel are due to the peak shifts that occurred depending on the intensity increase of the peaks belonging to the CS and β -CD. These changes indicating the chemical interaction of the β -CD and the CS confirm the synthesis of the CS-g- β -CD hydrogel. The peaks at 752 and 705 cm^{-1} belonging to the β -CD are not seen in the region of peaks between 850 - 700 cm^{-1} of FTIR spectra of the CS-g- β -CD hydrogel. These changes also show and confirm the synthesis of the CS-g- β -CD hydrogel.

An increase in the number and intensity of the peaks in the IR spectra of the Tenofovir disoproxil fumarate-loaded hydrogel was observed (Figure 3d). The absorption peak, which belong to the CS, observed around 1636 cm^{-1} in the empty hydrogel, increased to 1641 cm^{-1} in the spectra of the drug-loaded hydrogel, while the peak observed at 1549 cm^{-1} was reduced to 1545 cm^{-1} . The intensity of the absorption band appeared at 1257 cm^{-1} in the FTIR spectra of the empty hydrogel increased to 1261 cm^{-1} in the antiviral drug-loaded hydrogel. The interaction between the hydrogels and drug molecules was confirmed by the peak shifts observed in the IR spectra of the drug-loaded hydrogel. Malik et al. [48] observed slight shifts in the peaks of pure compounds forming the polymeric structure and some new peaks in the polymeric structure in the FTIR spectra of CS hydrogels loaded with the antiviral drug acyclovir. The authors noted that these changes represent the presence of acyclovir in the synthesized hydrogel and indicate the compatibility of the polymeric network with the antiviral drug acyclovir. The new absorption peak emerged at 1755 cm^{-1} in the IR spectra of the tenofovir disoproxil fumarate loaded hydrogel is due to the ester bonds in the structure of the drug molecules. Additionally, the peaks between 651 cm^{-1} and 1024 cm^{-1} , which are not seen in the empty hydrogel, in the spectrum of the drug-loaded hydrogel, are thought to belong to drug molecules that did not interact with the hydrogel.

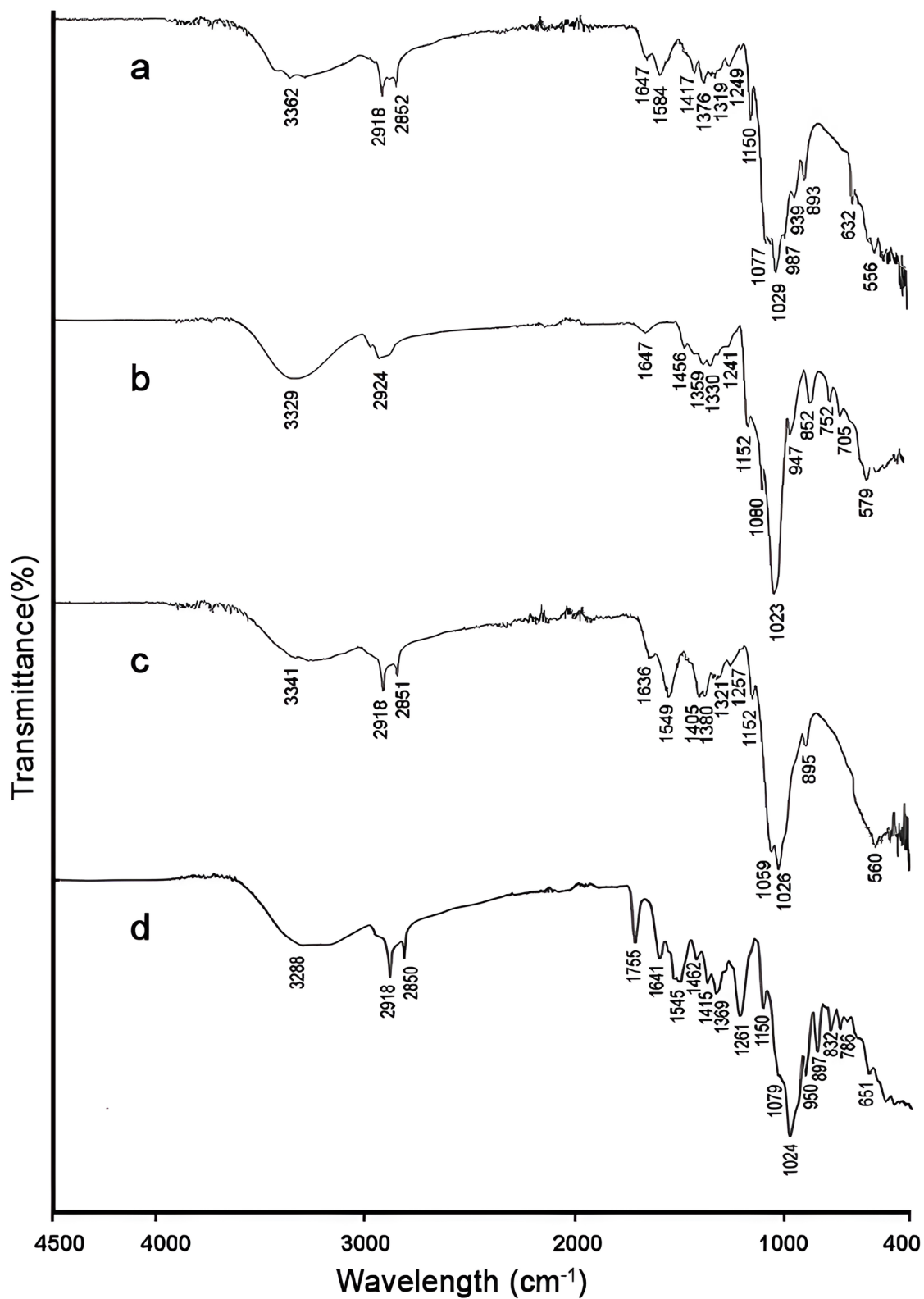


Figure 3. FTIR spectra of the synthesized hydrogel and its raw materials a) Crayfish CS, b) β -CD, c) CS-g- β -CD hydrogel d) Drug (0.04 g) loaded CS-g- β -CD hydrogel.

SEM Analysis Results of Hydrogels

The empty hydrogel exhibited a porous and reticulated structure with a nearly homogeneous mesh size (Figure 4a). TDF loaded hydrogel, on the other hand, exhibits more like lamellar structure (Figure 4b). Zhou et al. [26] reported that loading drug in the CS- β -cyclodextrin (CS- β -CD) hydrogel changed the morphology of the empty hydrogel having regular structure, making it irregular and the hydrogel exhibited a distinct lamellar structure. In this study, the CS-g- β -CD hydrogel became more irregular, compact, and fractured after loading with TDF. Paun et al. [46] have observed aggregation in the SEM image of the CS/ β -CD composite membrane, which they developed to encapsulate the gallic acid and ensure its controlled release, due to the poor distribution of the gallic acid in the chitosan solution. Malik et al. [48] observed the drug crystals on the surface of the β -cyclodextrin-CS-based hydrogels due to the migration of drug particles to the surface with water during drying. In this study, however, in the SEM image of the antiviral drug-loaded hydrogel, no drug molecules migrating to the surface or any aggregation of the drug molecules were observed.

XRD Analysis Result of Hydrogels

XRD motifs of the empty and the drug-loaded CS-g- β -CD hydrogels are seen in the Figure 5. A single broad amorphous peak around $2\theta=20^\circ$ was observed in the XRD spectra of the blank CS-g- β -CD hydrogel (Figure 5a). The XRD spectra of the TDF-loaded CS-g- β -CD hydrogel indicated two amorphous peaks, one small and one large, around 11° and 21° (Figure 5b). However, when the chitosan is cross-linked with the glutaraldehyde to form a hydrogel, the ability of the chitosan to form intra- and inter-molecular hydrogen bonds decreases, and the crystal structure of the polymer changes [49]. Moreover, the haphazard occurrence of the grafting process along the polymeric backbone causes the destruction of intermolecular hydrogen bonds [50]. Therefore, the CS-g- β -CD hydrogel exhibits a more amorphous structure with weak and low-intensity peaks. A study has reported that the XRD spectra of CS nanoparticles obtained from shrimp shells showed two peaks at 10° and 20° [51]. These peaks have disappeared after cross-linking of CS nanoparticles with tripolyphosphate (TPP) and the XRD spectra exhibited an amorphous structure. In this study, the XRD spectra of CS-g- β -CD hydrogels cross-linked with glutaraldehyde showed an amorphous structure.

The XRD spectrum of the antiviral drug TDF, on the other hand, exhibits a highly crystalline structure due to the molecules it contains (Figure 5c). It shows multiple and sharp peaks representing the crystalline structure. These observations confirming the crystalline nature of the TDF were also reported by Elionai et al. [52] for the TDF (two intense peaks at $2\theta = 20^\circ$ and 25° and other various peaks at 10° , 18° , 22° , 28° , and 30°). The model antiviral drug acyclovir also exhibited sharp, intense and characteristic peaks at 18.50° , 21.50° and 30.50° in the XRD spectrum [48], similar to those in this study.

However, the TDF showed no peaks after loading onto the CS-g- β -CD hydrogel. The X-ray spectrum of the TDF-loaded CS-g- β -CD hydrogel showed two broad bands around $2\theta = 11^\circ$ and 21° . This reveals the amorphous profile of the hydrogel. The disappearance of the TDF characteristic peaks in the XRD spectrum of the CS-g- β -CD hydrogel indicates that the drug cannot form crystals and its molecular distribution within the formed polymeric network during hydrogel synthesis [53].

In a previous study, the XRD spectrum of the β -CD was reported to exhibit an amorphous structure with 2 broad peaks around 10° and 20° [54]. The authors noted that while the scutellarin/ β -CD complex shows an amorphous XRD spectrum, it exhibits a halo pattern that is quite different due to the superimposition of the physical mixture of these two substances. This was due to the inclusion complex forming between scutellarin and β -CD. Another study reported that β -CD showed an amorphous structure with only one broad peak centered at 19.5° , while XRD patterns of myricetin exhibited some sharp peaks and the compound showed crystalline structure [45]. However, the authors stated that the XRD motifs of the β -CD/myricetin complex exhibit an amorphous structure, displaying typical halo patterns, which is an indication that myricetin is fully incorporated into the β -CD space. The XRD model of the TDF loaded CS-g- β -CD hydrogel in this study is similar to the findings in the above references.

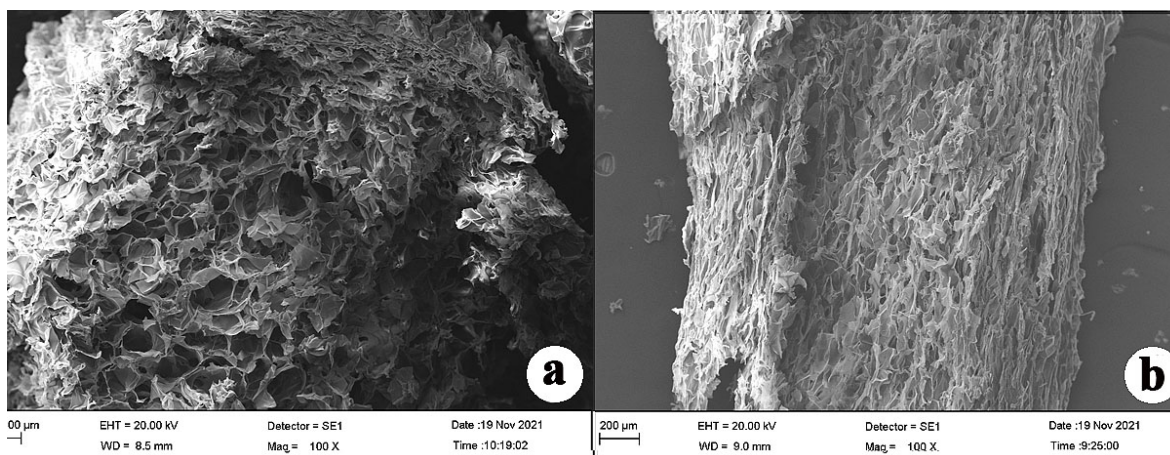


Figure 4. SEM images of the CS-g-β-CD hydrogel (a), and the drug (0.04 g) loaded CS-g-β-CD hydrogel (b).

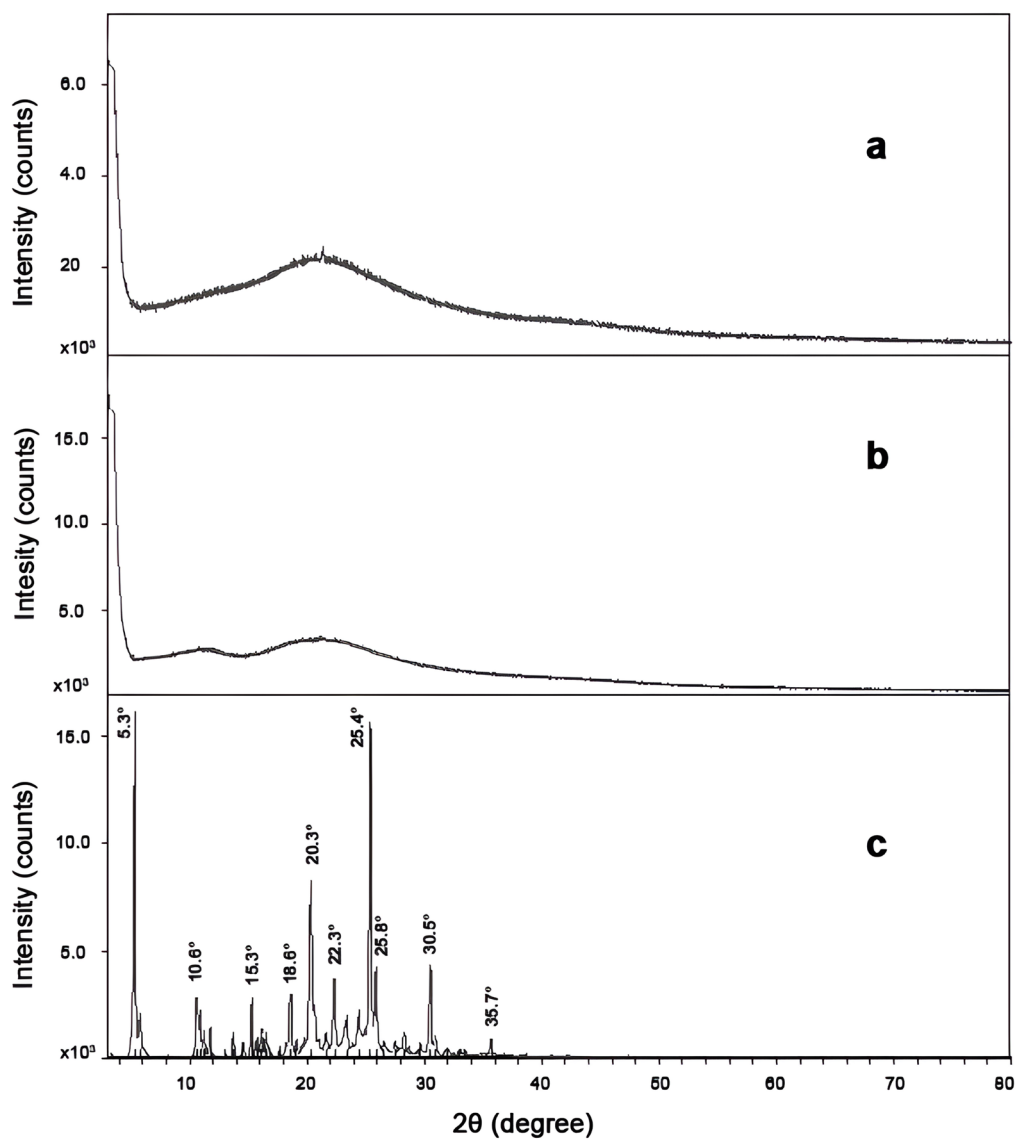


Figure 5. XRD graphs of the blank CS-g-β-CD hydrogel (a), the antiviral drug TDF (0.04g) loaded hydrogel (b), and the Tenofvir disoproxil fumarate (c).

¹H-NMR Analysis Result of Hydrogels

¹H-NMR spectroscopy analysis was employed to reveal the composition of the synthesized hydrogel and to confirm the interaction of the hydrogel with the antiviral drug (Figure 6 and Figure 7). In the NMR spectrum of the CS-g-β-CD hydrogel, the long peak observed around 7.27 ppm belongs to CDCl₃ (Deuteriochloroform) used as solvent (Figure 6a). Deuteriochloroform used as solvent in ¹H-NMR analysis gave a signal at 7.26 ppm [55]. The decreased signal observed around 10 ppm is due to glutaraldehyde. Lopez-Cervantes et al. [56] observed the proton signals of the aldehyde group of the glutaraldehyde at 9.6 ppm in the ¹H-NMR spectrum of chitosan glutaraldehyde biosorbent, in which they used deuterium hydrochloride as a solvent. In addition, hydrogens belonging to the N-acetyl group of the CS gave signals around 2 ppm. The signals of protons belonging to the glucosamine and N-acetylglucosamine groups of the CS showed a shift of around 3 ppm and gave weak signals between 3 ppm and 4 ppm. It was reported by Lopez-Cervantes et al. [56] that the acetyl group of the CS gave signals around 1.8 ppm, while the H-3–H-6 protons of the D-glucosamine and N-acetylglucosamine groups gave split signals around 3.4 and 3.8 ppm. The authors also observed a visible signal at 3 ppm and a single signal at 1.8 ppm for the H-2 proton of the D-glucosamine fraction. They also pointed out that the intensity of the peaks at 3.0–3.8 ppm decreased indicating the cross-linking of the glucosamine groups of the CS with glutaraldehyde. The H-2 proton gave signals at 2.68 ppm in the NMR spectra of the CS, while the H-3 to H-6 protons gave multiple signals in the range of 3.85–3.55 ppm [57]. The NMR signal around 1 ppm belonging to the β-CD belongs to the CH₃ protons (Figure 6a). In addition, the peaks between 3 ppm and 4 ppm indicate the signals belonging to the β-CD, and the glucosamine

and N-acetylglucosamine groups of the CS. Since the CS and the β-CD are both carbohydrate derivatives, it is possible that the signals of their protons may be close to each other or overlap. The proton signal of the β-CD at 1 ppm originates from the CH₃ group [58]. In addition, the authors reported that H-2, H-4 protons of the β-CD signaled around 3.5 ppm, while H-1, H-3, H-5, and H-6 protons gave weak signals between 4.5–5 ppm. Evangelista et al. [28] observed that the ¹H-NMR spectrum of the CS/β-CD complex give signals belonging to both CS and β-CD between 2 ppm and 5.5 ppm.

As the antiviral drug had a complex chemical composition, numerous and diverse signals stand out in the NMR spectra (Figure 6b). The NMR spectrum of the TDF showed strong and split peaks around 1.4 ppm, multiple multi-proton signals between 3.8 and 6 ppm, strong single proton signals at 7.2 ppm, and weak double and triple signals at 8.4 ppm. In the ¹H-NMR spectra of the TDF, Sichilongo et al. [59] recorded doublet signals at 1 ppm, 1.2 ppm, 3.9 ppm, 4 ppm, and 4.2 ppm, multiple signals at 4.8 ppm, and singlet signals at 5.5 ppm, 6.6 ppm, 7.2 ppm, 8 ppm and 8.1 ppm.

The ¹H-NMR spectra of the CS-g-β-CD hydrogel loaded with the TDF (0.04 g) is shown in Figure 7. In this study, ¹H-NMR spectra of TDF and CS-g-β-CD hydrogels loaded with this drug showed almost identical signals. The NMR spectrum of the TDF-loaded hydrogel reveals that the drug is stored in the CS-g-β-CD hydrogel and the interactions between the hydrogel and drug molecules are physical. It probably indicates inclusion complexes that the β-CD may have formed with the antiviral drug. A significant upshift in the signals of H-3 proton (3.7396 ppm) and H-5 proton (3.6145 ppm) located in the interior cavity of the β-CD is attributed to the inclusion complexing of the β-CD with drug molecules [60].

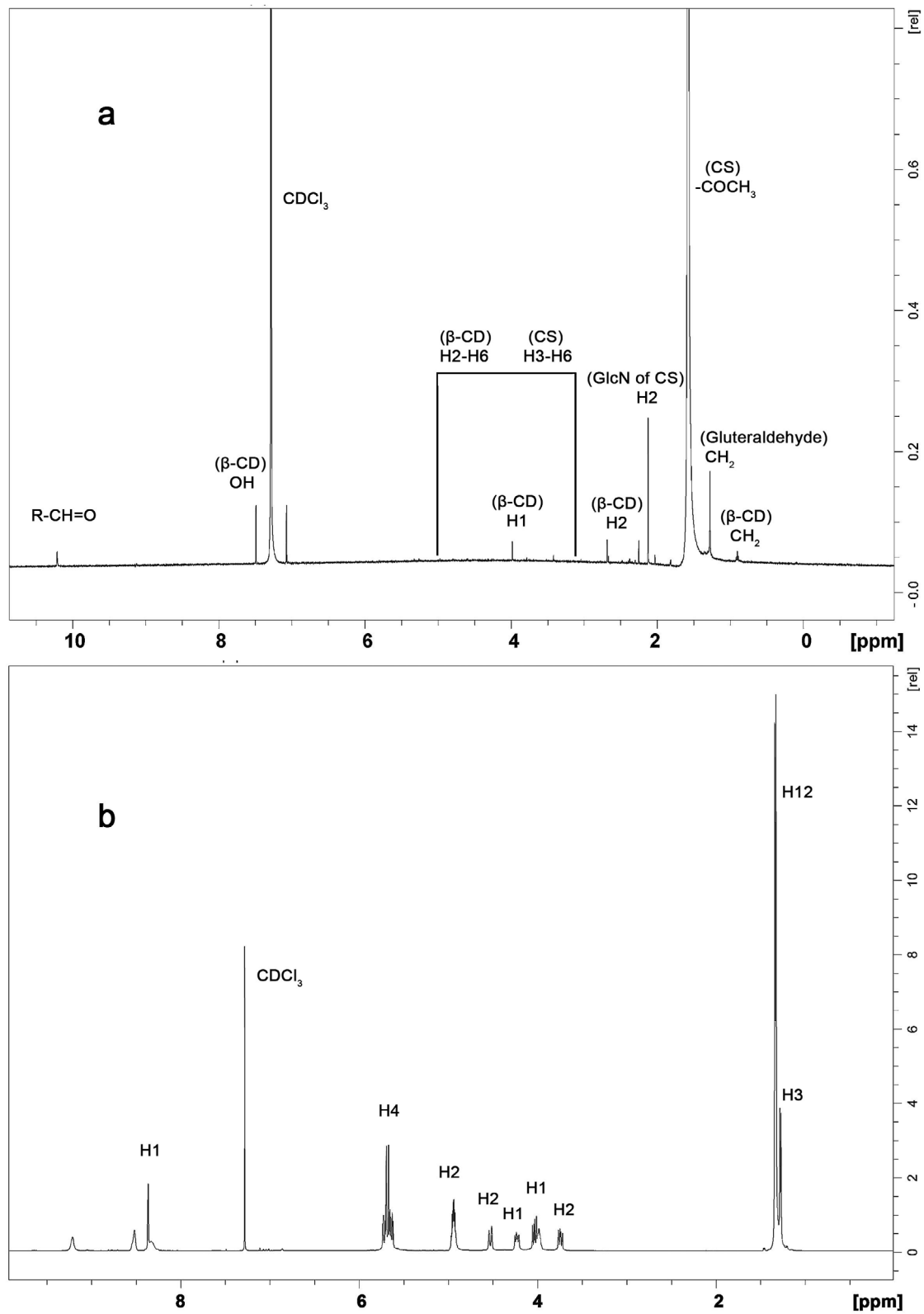


Figure 6. NMR spectra of a) CS-g-β-CD hydrogel, and b) Tenofovir disoproxil fumarate.

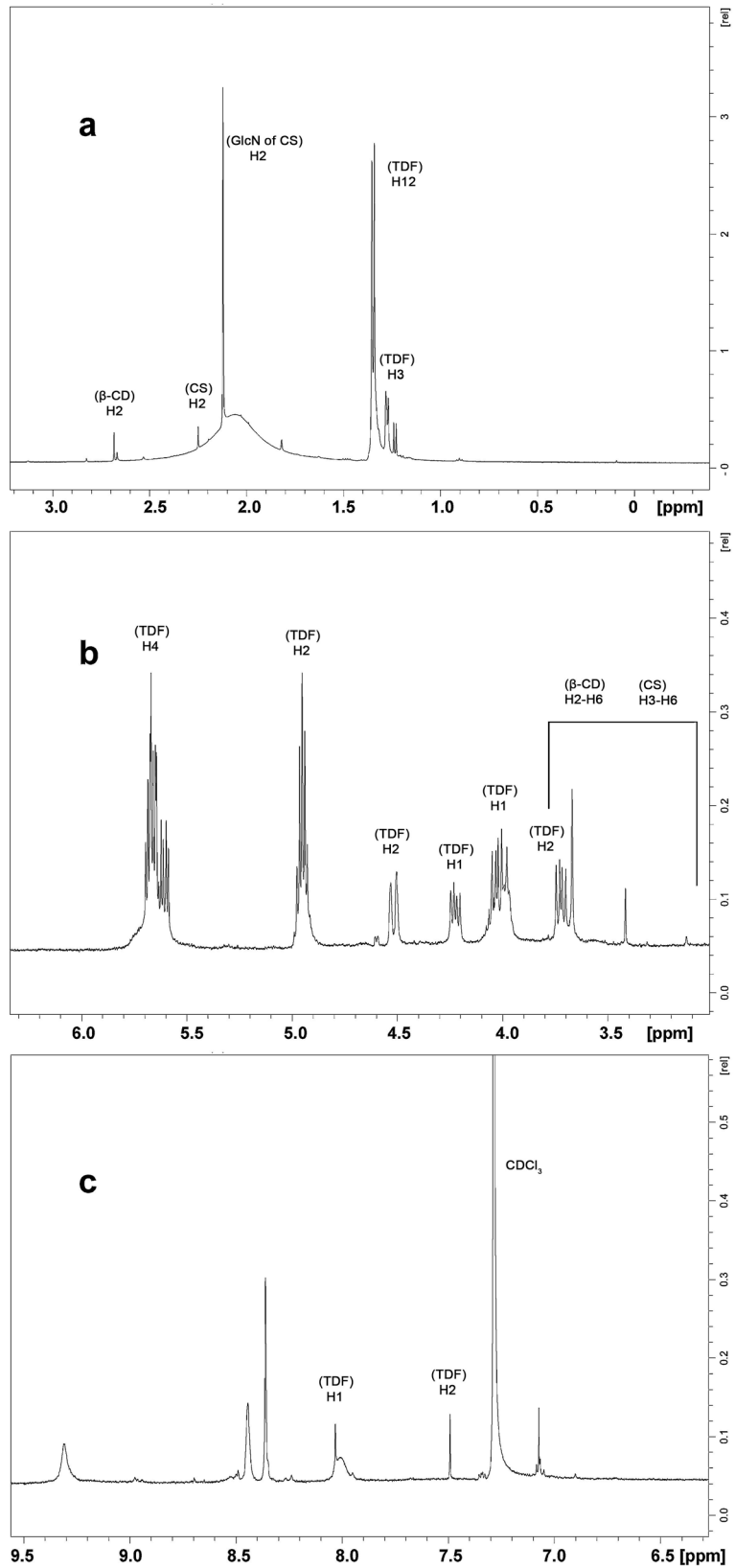


Figure 7. NMR spectra of the Tenofovir disoproxil fumarate (0.04 g) loaded CS-g-β-CD hydrogel.

Functionality Test Results of the Synthesized CS-g- β -CD Hydrogels

Gelation and Swelling Percentage of the CS-g- β -CD Hydrogels

The percentage gelation of the synthesized hydrogels are presented in Table 1. The gelation percentages of the synthesized hydrogels varied between 52.49% and 90.38%. The increase in the amount of the β -CD results in a decrease in the gelation function from monomer to gel [61].

The CS-g- β -CD hydrogel containing 0.04 g of the β -CD swelled 18.9-21.74 times its dry weight in distilled water. The swelling capacity of the CS-g- β -CD hydrogels increased depending on the amount of β -CD. The equilibrium swelling percentages were found to be 728.1%, 937.9%,

1441.5% and 2074.1% for G0, G1, G2 and G3, respectively. The β -CD has a lot of $-\text{OH}$ and $-\text{CH}_2\text{OH}$ groups and these groups enable the hydrophilicity to the hydrogels. These functional groups are ionized at pH 7.4, and lead to an increase in electrostatic repulsive forces and provide a more expanded configuration. This enlarged configuration with the higher amount of β -CD in the prepared hydrogel causes an increase in water uptake and swelling [61,62].

Standard Calibration Curve of the Antiviral Drug

The maximum absorbance value (λ_{max}) for the TDF solution was determined as 261 nm. The calibration curve of the drug was prepared using the values obtained by reading the drug solutions at various concentrations (ppm) at a wavelength of 261 nm in a UV spectrophotometer (Figure 8).

Table 1. Gelation percentage of the CS-g- β -CD hydrogels.

Hydrogel	Gelation (%)
G0	90.38%
G1	78.99%
G2	72.72%
G3	52.49%

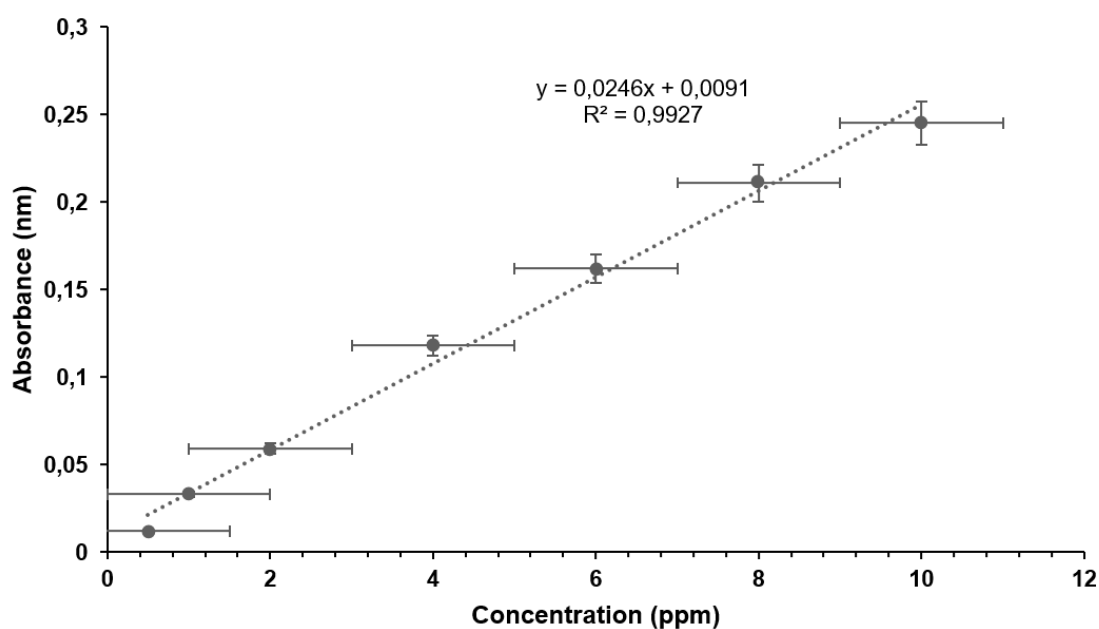


Figure 8. Calibration curve of the Tenofovir diproxil fumarate.

TDF release from the CS-g- β -CD hydrogel

TDF release behaviors of the synthesized hydrogels in PBS solution (pH 7.4) are given in Figure 9. In the TDF-loaded CS-g- β -CD hydrogels, drug release occurred from the first minutes as the gel started to swell, and the drug release amount gradually increased depending on time and reached equilibrium at 24 hours. In Figure 9, the TDF release from the G3 hydrogel containing the highest amount of β -CD started with a burst rapid of 58.75% drug release within the first 15 minutes and then continued a steady slower release up to 63% within 60 minutes. After 24 hours, 73% of the TDF loaded to the CS-g- β -CD hydrogel could be released in PBS solution at equilibrium. On the contrary, Figure 9 indicates that the drug release of pure CS (G0) is higher than that of CS-g- β -CD (G3) hydrogels. This can be due to the increase in the diffusional path depending on the high swelling capacity of the CS-g- β -CD hydrogels. Hydrophobic drug TDF was found to be retained within the hydrogel structure despite extensive washing with DMSO or methanol. Hydrogels are suitable candidates as carriers for poorly water-soluble drugs to improve their solubility [27,62].

The TDF release mechanism of the synthesized CS-g- β -CD hydrogels was examined by fitting the data obtained from the first 60% drug release to the Korsmeyer-Peppas model [63]. The drug release kinetics of all the synthesized CS-g- β -CD hydrogels were examined by Korsmeyer-Peppas, zero-order, Higuchi, and first-order models. All the models showed a similar trend with the TDF release data. The regression coefficient (R^2) is frequently used to discover whether a kinetic model fits the drug release data and the strength of the tested models. Therefore, the model that best fits the release data was selected based on the R^2 value being close to 1. Table 2 illustrates that Korsmeyer-Peppas model better fitted the release of TDF ($R^2 > 0.99$) than the other models. The Korsmeyer-Peppas kinetic model is a semi-empirical model that can describe the drug release behaviors through diffusion or swelling [64]. In this model, in order to evaluate the release mechanism, the diffusion constant (n) value, which indicates the type of release mechanism, is calculated. For cylindrical samples, $n < 0.45$ indicates pseudo-Fickian diffusion (diffusion-controlled), $0.45 < n < 0.89$ indicates non-Fickian diffusion (abnormal drug release/diffusion and erosion controlled), $n = 0.89$ indicates Case II (polymer relaxation-controlled), and $n > 0.89$ indicates supercase II [63].

In this study, the n value was found to be between 0.2712-0.2956, indicating a pseudo-Fickian diffusion. This shows a rapid diffusion of water into the hydrogel but the equilibrium is reached very slowly [36].

A study reported that considering R^2 , k , and n values, drug release from the chitosan films best fit the zero-order kinetic model, indicating a sustained drug release [65]. Another study has reported that the acyclovir (ACV) release kinetics of the chitosan- β -cyclodextrin-based hydrogel best fit the Peppas model ($R^2 = 0.9651$ and n value: 0.2681) [66]. In the study, it has been suggested that the drug release mechanism may be due to drug diffusion from pores in the hydrogel through the partially swollen hydrogel matrix. Suhail et al. [67] stated that all formulations of the chitosan- β -cyclodextrin polyacrylamide (CS/ β -CDcPAA) hydrogel they developed, followed the first-order model and the n values were between 0.5228 and 0.6310, representing a non-Fickian diffusion. The authors pointed out that for the CS/ β -CDcPAA hydrogel, the key factor affecting the loading and release of drugs is the swelling index. Malik et al. [48] found that the release of Acyclovir (ACV) from β -cyclodextrin/chitosan/methacrylic acid (β -CD/CS-co-poly(MAA)) hydrogels followed zero-order kinetics. The authors observed that the n values determined from the drug release data of the ACV-containing hydrogels followed the Fickian mechanism in the release into the simulated gastric fluid and the non-Fickian mechanisms in the release into the simulated intestinal fluid, and they emphasized that the drug release rate from the hydrogels shows the swelling behavior of the gel.

The zero-order drug release is continuous and time-dependent and describes single-phase drug release from a hydrogel system that releases its content at a constant rate not related to the concentration [64]. It can be observed in materials with swelling ability [68]. In the first-order model, the release kinetics depend on the initial concentration and show a much slower and different release rate over time depending on the remaining drug concentration [69]. The amount of the released drug is proportional to the square root of time in the Higuchi model [63]. In this study, considering the R^2 and n values, all formulations of the CS-g- β -CD hydrogel best fit the Korsmeyer-Peppas model, which describes different release events including diffusion or swelling, and were not compatible with the models mentioned above (Table 2, Figure 9).

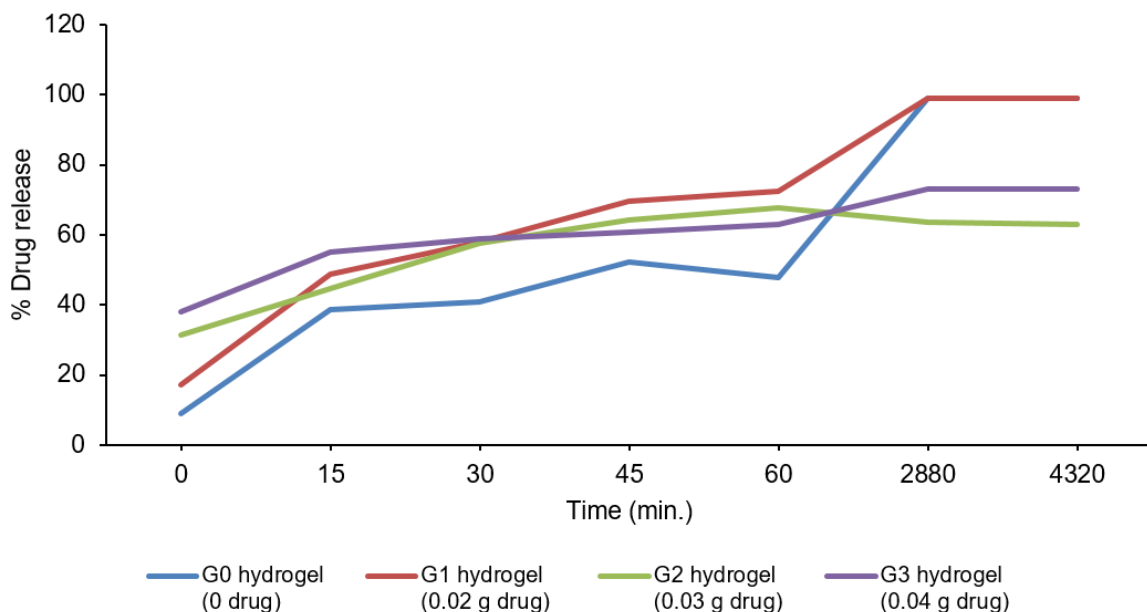


Figure 9. Drug release profile of the G0-G3 hydrogels at pH 7.4, and 37°C.

Table 2. TDF release characteristics of the prepared hydrogelst.

Kinetik models	Parameters (%)	G0	G2	G3
Zero order kinetics	K_0 (min^{-1})	0.0072	0.0075	0.0021
	R^2	0.9502	0.9497	0.9765
First-order kinetics	K_1 (min^{-1})	0.0802	0.0102	0.0066
	R^2	0.9565	0.9757	0.9878
Higuchi model	K_2 (min^{-1})	0.0826	0.0553	0.0244
	R^2	0.9449	0.9632	0.9979
Korsmeyer- Peppas model	n	0.2712	0.2860	0.2956
	k	0.196	0.321	0.483
	R^2	0.9504	0.9920	0.9906

CONCLUSION

In this study, the CS-g- β -CD hydrogels were synthesized in a single step for the controlled release of the TDF using the crayfish chitosan and β -Cyclodextrin which are natural biomaterials. The addition of β -CD to the CS hydrogel improved the swelling behavior of the hydrogel and the controlled release of TDF from the hydrogel due to the formation of the host-guest complex. The hydrophobic drug TDF was found to be retained within the hydrogel structure although extensive washing with DMSO was carried out. This shows the suitability of the CS-g- β -CD hydrogels for the delivery of the hydrophobic drug TDF having low bioavailability. The TDF release

kinetics of the CS-g- β -CD hydrogels are better fitted to the Korsmeyer-Peppas model ($r^2 > 0.99$) suggesting a diffusion-controlled release mechanism through the partially swollen hydrogel matrix and pores in the hydrogel.

CS-g- β -CD hydrogel has the potential to be a suitable drug delivery system for other hydrophobic antiviral drugs as well as TDF used in the treatment of diseases that require lifelong drug use, such as HIV and Hepatitis B. Moreover, the synthesized CS-g- β -CD hydrogel may offer an opportunity to develop a new drug delivery system as a temporary wound dressing and as a mucoadhesive hydrogel for transdermal drug delivery and cosmetic applications.

Acknowledgement:

This work was supported by the Trakya University Scientific Research Projects Unit within the scope of the research project, No: TUBAP 2020/149. The authors thank Nobel İlaç San. ve Tic. A.Ş. (Turkey) for supplying the active substance Tenofovir disoproxil fumarate.

References

- WHO, 2021a. "World Health Organisation, Coronavirus (COVID-19)", <https://covid19.who.int/> (Erişim tarihi: 29.10.2021)
- K. Kurt, L. Dönbak, A. Kayraldız, Tenofovir Disoproxil Fumarate in the Treatment of AIDS, *Archives Medical Review Journal*, 24 (2015) 119-134.
- WHO, 2021b. "World Health Organisation, Hepatitis B", <https://www.who.int/news-room/fact-sheets/detail/hepatitis-b> (Erişim tarihi: 29.10.2021)
- UNAIDS, 2021. "The Joint United Nations Programme on HIV/AIDS, Global HIV & AIDS statistics-Fact sheet", <https://www.unaids.org/en/resources/fact-sheet> (Erişim tarihi: 02.12.2021)
- D. Yu, J. Heathcote, Tenofovir in the treatment of chronic hepatitis B, *Therapy*, 8 (2011) 527-544.
- J.E. Gallant, S. Deresinski, Tenofovir disoproxil fumarate, *Clin. Infect. Dis.*, 37 (2003) 944-950.
- S.M. Ecin, N. Çalık Başaran, M. Aladağ, Evaluation of the effectiveness of tenofovir in chronic hepatitis B patients, *acta medica*, 51 (2020) 9-14.
- J. Li, D.H. Zhang, X.X. Zhang, The Occurrence of rtA194T Mutant After Long-Term Lamivudine Monotherapy Remains Sensitive to Tenofovir Disoproxil Fumarate: A Case Report, *Infect. Drug Resist.*, 14 (2021) 1013-1017.
- S. Selvaraj, V. Niraimathi, M. Nappinnai, Formulation and evaluation of acyclovir loaded chitosan nanoparticles, *Int. J. Pharm. Anal. Res.*, 5 (2016) 619-629.
- M.M. Al-Tabakha, S.A. Khan, A. Ashames, H. Ullah, K. Ullah, G. Murtaza, N. Hassan, Synthesis, Characterization and Safety Evaluation of Sercin-Based Hydrogels for Controlled Delivery of Acyclovir, *Pharmaceuticals*, 14 (2021) 234.
- N.S. Malik, M. Ahmad, M.U. Minhas, R. Tulain, K. Barkat, I. Khalid, Q. Khalid, Chitosan/Xanthan Gum Based Hydrogels as Potential Carrier for an Antiviral Drug: Fabrication, Characterization, and Safety Evaluation, *Front. Chem.*, 8 (2020) 50.
- L.J. del Valle, A. Diaz, J. Puiggali, Hydrogels for biomedical applications: cellulose, chitosan, and protein/peptide derivatives, *Gels*, 3 (2017) 27.
- H. Kono, T. Teshirogi, Cyclodextrin-grafted chitosan hydrogels for controlled drug delivery, *Int. J. Biol. Macromol.*, 72 (2015) 299-308.
- Y. Moukbil, F.N. Oktar, B. Ozbek, D. Ficai, A. Ficai, E. Andronescu, M. Sayip Eroğlu, O. Gunduz, Biohydrogels for medical applications: A short review, *Org. Commun.*, 11 (2018) 123-141.
- S. Peers, A. Montebault, C. Ladaviere, Chitosan hydrogels for sustained drug delivery, *J. Control. Release*, 326 (2020) 150-163.
- R.C.F. Cheung, T.B. Ng, J.H. Wong, W.Y. Chan, Chitosan: An Update on Potential Biomedical and Pharmaceutical Applications, *Mar. Drugs*, 13 (2015) 5156-5186.
- F.S. El-banna, M.E. Mahfouz, S. Leporatti, M. El-Kemary, N.A.N. Hanafy, Chitosan as a Natural Copolymer with Unique Properties for the Development of Hydrogels, *Appl. Sci-Basel.*, 9 (2019) 2193.
- D. Zhao, S. Yu, B. Sun, S. Gao, S. Guo, K. Zhao, Biomedical Applications of Chitosan and Its Derivative Nanoparticles, *Polymers*, 10 (2018) 462.
- E.S. Abdou, K.S.A. Nagy, M.Z. Elsabee, Extraction and characterization of chitin and chitosan from local sources, *Bioresour. Technol.*, 99 (2008) 1359-1367.
- S.S.A. Loutfy, M.H. Elberry, K.Y. Farroh, H.T. Mohamed, A.A. Mohamed, E.B. Mohamed, A.H.I. Faraag, S.A. Mousa, Antiviral Activity of Chitosan Nanoparticles Encapsulating Curcumin Against Hepatitis C Virus Genotype 4a in Human Hepatoma Cell Lines, *Int. J. Nanomedicine*, 15 (2020) 2699-2715.
- S. Mizrahy, D. Peer, Polysaccharides as building blocks for nanotherapeutics, *Chem. Soc. Rev.*, 41 (2012) 2623-2640.
- J.X. Zhang, P.X. Ma, Cyclodextrin-based supramolecular systems for drug delivery: Recent progress and future perspective, *Adv. Drug Deliv. Rev.*, 65 (2013) 1215-1233.
- P. Saokham, C. Muankaew, P. Jansook, T. Loftsson, Solubility of Cyclodextrins and Drug/Cyclodextrin Complexes, *Molecules*, 23 (2018) 1161.
- C.A.R. Barragán, E.R.M. Balleza, L. García-Uriostegui, J.A.A. Ortega, G. Toriz, E. Delgado, Rheological characterization of new thermosensitive hydrogels formed by chitosan, glycerophosphate, and phosphorylated β -cyclodextrin, *Carbohydr. Polym.*, 201 (2018) 471-481.
- S.A. Khan, W. Azam, A. Ashames, K.M. Fahalebom, K. Ullah, A. Mannan, G. Murtaza, β -Cyclodextrin-based (IA-co-AMPS) Semi-IPNs as smart biomaterials for oral delivery of hydrophilic drugs: Synthesis, characterization, in-Vitro and in-Vivo evaluation, *J. Drug Deliv. Sci. Technol.*, 60 (2020) 101970.
- H.Y. Zhou, Z.Y. Wang, X.Y. Duan, L.J. Jiang, P.P. Cao, J.X. Li, J.B. Li, Design and evaluation of chitosan- β -cyclodextrin based thermosensitive hydrogel, *Biochem. Eng. J.*, 111 (2016) 100-107.
- K. Yang, S. Wan, B. Chen, W. Gao, J. Chen, M. Liu, B. He, H. Wu, Dual pH and temperature responsive hydrogels based on beta-cyclodextrin derivatives for atorvastatin delivery, *Carbohydr. Polym.*, 136 (2016) 300-6.
- T.F.S. Evangelista, G.R.S. Andrade, K.N.S. Nascimento, S.B. dos Santos, M.F. Coata Santos, C.R.M. Doca, C.S. Estevam, I.F. Gimenez, L.E. Almeida, Supramolecular polyelectrolyte complexes based on cyclodextrin-grafted chitosan and carrageenan for controlled drug release, *Carbohydr. Polym.*, 245 (2020) 116592.
- N.S. Malik, M. Ahmad, M.U. Minhas, Cross-linked β -cyclodextrin and carboxymethyl cellulose hydrogels for controlled drug delivery of acyclovir, *PLoS ONE*, 12 (2017) e0172727.
- W. Wang, S. Bo, S. Li, W. Qin, Determination of the Mark-Houwink Equation for Chitosans with Different Degrees of Deacetylation, *Int. J. Biol. Macromol.*, 13 (1991) 281-285.
- A. Rasool, S. Ata, A. Islam, M. Rizwan, M.k. Azeem, A. Mehmood, R.U. Khan, A.R. Qureshi, H.A. Mahmood, Kinetics and controlled release of lidocaine from novel carrageenan and alginate-based blend hydrogels, *Int. J. Biol. Macromol.*, 147 (2020) 67-68.
- N.R. Vyavahare, M.G. Kulkarni, M.R.A. Zero order release from hydrogels, *J. Membr. Sci.*, 54 (1990) 221-228.

33. H. Hosseinzadeh, Novel interpenetrating polymer network based on chitosan for the controlled release of cisplatin, *JBASR*, 2 (2012) 2200-2203.
34. S. Khan, N.M. Ranjha, Effect of degree of cross-linking on swelling and on drug release of low viscous chitosan/poly(vinyl alcohol) hydrogels, *Polym. Bull.*, 71 (2014) 2133-2158.
35. P.L. Ritger, N.A. Peppas, A simple equation for description of solute release I. Fickian and non-fickian release from non-swelling devices in the form of slabs, spheres, cylinders or discs, *J. Control. Release*, 5 (1987) 23-36.
36. S. Morariu, M. Bercea, L.M. Gradinaru, I. Rosca, M. Avadanei, Versatile poly(vinyl alcohol)/clay physical hydrogels with tailorable structure as potential candidates for wound healing applications, *Mat. Sci. Eng. C-Mater.*, 109 (2020) 110395.
37. M. Kaya, F. Dudakli, M. Asan-Ozusaglam, Y.S. Cakmak, T. Baran, A. Menten, S. Erdogan, Porous and nanofiber alpha-chitosan obtained from blue crab (*Callinectes sapidus*) tested for antimicrobial and antioxidant activities, *Lwt-Food Sci. Technol.*, 65 (2016) 1109-1117.
38. S. Erdogan, Textile finishing with chitosan and silver nanoparticles against *Escherichia coli* ATCC 8739, *Trak. Univ. J. Nat. Sci.*, 21 (2020) 21-32.
39. G. Michailidou, E.N. Koukaras, D.N. Bikiaris, Vanillin chitosan miscible hydrogel blends and their prospects for 3D printing biomedical applications, *Int. J. Biol. Macromol.*, 192 (2021) 1266-1275.
40. L.C. Gomes, S.I. Faria, J. Valcarcel, J.A. Vazquez, M.A. Cerqueira, L. Pastrana, A.I. Bourbon, F.J. Mergulhao, The Effect of Molecular Weight on the Antimicrobial Activity of Chitosan from *Loligo opalescens* for Food Packaging Applications, *Mar. Drugs*, 19 (2021) 384.
41. S.M. Joseph, S. Krishnamoorthy, R. Paranthaman, J.A. Moses, C. Anandharamakrishnan, A review on source-specific chemistry, functionality, and applications of chitin and chitosan, *Carbohydr. Polym. Technol. Appl.*, 2 (2021) 100036.
42. I. Aranaz, A.R. Alcántara, M.C. Civera, C. Arias, B. Elorza, A.H. Caballero, N. Acosta, Chitosan: An Overview of Its Properties and Applications, *Polymers*, 13 (2021) 3256.
43. M. Rajabi, M. McConnell, J. Cabral, M.A. Ali, Chitosan hydrogels in 3D printing for biomedical applications, *Carbohydr. Polym.*, 260 (2021) 117768.
44. H.Y. Zhou, X.G. Chen, M. Kong, C.S. Liu, D.S. Cha, J.F. Kennedy, Effect of molecular weight and degree of chitosan deacetylation on the preparation and characteristics of chitosan thermosensitive hydrogel as a delivery system, *Carbohydr. Polym.*, 73 (2008) 265-273.
45. D. Han, Z. Han, L. Liu, Y. Wang, S. Xin, H. Zhang, Z. Yu, Solubility enhancement of myricetin by inclusion complexation with heptakis-O-(2-Hydroxypropyl)- β -cyclodextrin: A joint experimental and theoretical study, *Int. J. Mol. Sci.*, 21 (2020) 766.
46. G. Paun, E. Neagu, A. Tache, G.L. Radu, New type of chitosan/2-hydroxypropyl- β -cyclodextrin composite membrane for gallic acid encapsulation and controlled release, *Acta Chim. Slov.*, 61 (2014) 27-33.
47. E.M. Sultanova, M.K. Salakhutdinova, Y.I. Oshchepkova, A.M. Asrorov, M.J. Oripova, U.J. Ishimov, S.I. Salikhov, Chitosan Hydrogel Improves Bioavailability of Megosin, *Eur. Pharm. J.*, 67 (2019) 1-6.
48. N.S. Malik, M. Ahmad, M.S. Alqahtani, A. Mahmood, K. Barkat, M.T. Khan, U.R. Tulain, A. Rashid, β -cyclodextrin chitosan-based hydrogels with tunable pH-responsive properties for controlled release of acyclovir: design, characterization, safety, and pharmacokinetic evaluation, *Drug Deliv.*, 28 (2021) 1093-1108.
49. Y. Wang, J. Wang, Z. Yuan, H. Han, T. Li, L. Li, X. Guo, Chitosan cross-linked poly(acrylic acid) hydrogels: Drug release control and mechanism, *Colloids Surf. B.*, 152 (2017) 252-259.
50. X. Hu, L. Feng, W. Wei, et al, Synthesis and characterization of a novel semi-IPN hydrogel based on Salecan and poly(N,N-dimethylacrylamide-co-2-hydroxyethyl methacrylate), *Carbohydr. Polym.*, 105 (2014) 135-144.
51. M.E.A. Ali, M.M.S. Aboelfadl, A.M. Selim, H.F. Khalil, G.M. Elkady, Chitosan nanoparticles extracted from shrimp shells, application for removal of Fe(II) and Mn(II) from aqueous phases, *Sep. Sci. Technol.*, 53 (2018) 2870-2881.
52. E.C. Elionai, W.N. Mussel, J.M. Resende, S.L. Fialho, J. Barbosa, E. Carignani, M. Geppi, M.I. Yoshida, Characterization of tenofovir disoproxil fumarate and its behavior under heating, *Cryst. Growth Des.*, 15 (2015) 1915-1922.
53. M. Bajpai, S. Bajpai, P. Jyotishi, Water absorption and moisture permeation properties of chitosan/poly(acrylamide-co-itaconic acid) IPC films, *Int. J. Biol. Macromol.*, 84 (2016) 1-9.
54. Y.X. Wang, Y.P. Qin, Z.J. Kong, Y.J. Wang, L.L. Ma, Glutaraldehyde Cross-linked Silk Fibroin Films for Controlled Release, *Advances in Materials and Materials Processing IV, Pts 1 and 2*, 887-888 (2014) 541-546.
55. G.R. Fulmer, A.J.M. Miller, N.H. Sherden, H.E. Gottlieb, A. Nudelman, B.M. Stoltz, J.E. Bercau, Karen I. Goldberg, NMR Chemical Shifts of Trace Impurities: Common Laboratory Solvents, Organics, and Gases in Deuterated Solvents Relevant to the Organometallic Chemist, *Organometallics*, 29 (2010) 2176-2179.
56. J. López-Cervantes, D.I. Sánchez-Machado, R.G. Sánchez-Duarte, M.A. Correa-Murrieta, Study of a fixed-bed column in the adsorption of an azo dye from an aqueous medium using a chitosan-glutaraldehyde biosorbent, *Adsorp. Sci. Technol.*, 36 (2018) 215-232.
57. S. Chatterjee, P.C.L. Hui, C.W. Kan, W. Wang, Dual-responsive (pH/temperature) Pluronic F-127 hydrogel drug delivery system for textile-based transdermal therapy, *Sci. Rep.*, 9 (2019) 11658.
58. Z. Aytac, S.I. Kusku, E. Durgun, T. Uyar, Encapsulation of gallic acid/cyclodextrin inclusion complex in electrospun polylactic acid nanofibers: Release behavior and antioxidant activity of gallic acid, *Mater. Sci. Eng. C-Mater. Biol. Appl.*, 63 (2016) 231-239.
59. K. Sichilongo, Z.G. Keolopile, S. Ndlovu, E. Mwando Jr., C. Shaba, E. Massele, Characterization of tenofovir, tenofovir disoproxil fumarate and emtricitabine in aqueous solutions containing sodium ions using ESI-MS, NMR and Ab initio calculations, *Int. J. Mass Spectrom.*, 410 (2016) 1-11.
60. G. Yurtdaş Kirmiziloğlu, Host-guest inclusion complex of desloratadine with 2(hydroxy)propyl- β -cyclodextrin (HP- β -CD): Preparation, binding behaviors and dissolution properties, *J. Res. Pharm.*, 24 (2020) 693-707.
61. B. Tasdelen, N. Kayaman-Apohan, O. Güven, B.M. Baysal, Swelling and diffusion studies of poly(N-isopropylacrylamide/itaconic acid) copolymeric hydrogels in water and aqueous solutions of drugs, *J. Appl. Polym. Sci.*, 91 (2004) 911-915.

62. T. Demirci, M. Erginer Hasköylü, M.S. Eroğlu, J. Hemberger, E. Toksoy Öner, Levan-based hydrogels for controlled release of Amphotericin B for dermal local antifungal therapy of Candidiasis, *Eur. J. Pharm. Sci.*, 145 (2020) 105255.
63. B. Nigusse, T. Gebre-Mariam, A. Belete, Design, development and optimization of sustained release floating, bioadhesive and swellable matrix tablet of ranitidine hydrochloride. *PLoS ONE*, 16 (2021) e0253391.
64. L.P. Jahromi, M. Ghazali, Hb. Ashrafi, A. Azadi, A comparison of models for the analysis of the kinetics of drug release from PLGA-based nanoparticles, *Heliyon*, 6 (2020) e03451.
65. G. Yasayan, Chitosan films and chitosan/pectin polyelectrolyte complexes encapsulating silver sulfadiazine for wound healing, *Istanbul J. Pharm.*, 50: (2020) 238-244.
66. H.Y. Zhou, Z.Y. Wang, X.Y. Duan, L.J. Jiang, P.P. Cao, J.X. Li, J.B. Li, Design and evaluation of chitosan- β -cyclodextrin based thermosensitive hydrogel, *Biochem. Eng. J.*, 111 (2016) 100-107.
67. M. Suhail, Y.F. Shao, Q.L. Vu, P.C. Wu, Designing of pH-Sensitive Hydrogels for Colon Targeted Drug Delivery; Characterization and In Vitro Evaluation, *Gels*, 8 (2022) 155.
68. N.S. Heredia, K. Vizuete, M. Flores-Calero, V.K. Pazmiño, F. Pilaquinga, B. Kumar et al, Comparative statistical analysis of the release kinetics models for nanoprecipitated drug delivery systems based on poly(lactic-co-glycolic acid), *PLoS ONE*, 17 (2022) e0264825.
69. J. Bhasarkar, D. Bal, Kinetic investigation of a controlled drug delivery system based on alginate scaffold with embedded voids, *J. Appl. Biomater. Funct. Mater.*, 17 (2019) 2280800018817462.